A large displacement orthotropic viscoelastic model for manufacturing-induced distortions in Fibre Metal Laminates

Abouhamzeh, M.; Sinke, J.; Benedictus, R.

DOI
10.1016/j.compstruct.2017.06.009

Publication date
2019

Document Version
Accepted author manuscript

Published in
Composite Structures

A large displacement orthotropic viscoelastic model for manufacturing-induced distortions in Fibre Metal Laminates

M. Abouhamzeh*

m.abouhamzeh@tudelft.nl, morteza.ab@gmail.com

J. Sinke

R. Benedictus

Faculty of Aerospace Engineering, Delft University of Technology, Kluyverweg 1, 2629 HS Delft, The Netherlands

*Corresponding author.

Abstract

Distortions and residual stresses are predicted in Fibre Metal Laminates (FMLs) under large deformations. A new modelling procedure is presented for small and large deformation analysis of thermo-viscoelastic problems of orthotropic materials. The material model is implemented in a finite element package which can be used for cure and/or temperature dependent response of composites undergoing large rotations but with small strains.

Temperature-dependent and viscoelastic responses are characterised for GLARE, as the mostly used type of FMLs. The geometrically nonlinear thermo-viscoelastic model is used to predict the manufacturing-induced warpage of panels. The curing stresses are calculated from a previously developed model accounting for chemical shrinkage and stiffness evolution of the prepreg layers during cure. The shape deviation of some non-symmetric GLARE panels are predicted and compared to the real measurement of fabricated laminates. The accuracy of the model is verified which can be used in further studies to improve the precision of manufacturing and assembly and also to have better prediction of the fatigue life and residual strength.

Keywords: GLARE; Glass-epoxy prepreg; Curing; Thermo-viscoelastic; Large-deformation

1 Introduction

Besides their high values of strength/weight ratios, alternating metal and composite layers in FMLs allow to obtain high structural performances like fatigue life, residual strength and damage tolerance. Glass Aluminium Reinforced Epoxy (GLARE) serves as the most common type which is being used in fuselage panels and leading edges of tail planes of Airbus A-380.

Research is being conducted at TU Delft, Faculty of Aerospace Engineering on the analysis and prediction of manufacturing processes on a fuselage panel made of GLARE. Preliminary modelling and experiments are already carried out to study the contribution of different mechanisms on the initiation of residual stress and distortion of GLARE samples [1,2]. The shape deviations should be predictable prior to manufacturing to be compensated in the tooling to achieve easy and accurate assembly. Knowing the residual stress values or possibly decreasing them, helps to achieve better structural responses in the service life of the material. The mould geometry can be adapted accordingly to produce (much) more accurate products and also minimise the residuals stresses of the panels.

Integrated GLARE panels are made by curing of prepreg layers (with glass fibres and epoxy adhesive) between aluminium sheets. Reinforcements like doublers and stringers would also be attached to the already cured laminates using a 2nd cure cycle. The epoxy adhesive in the prepreg layers of FMLs, behaves temperature dependent and viscoelastic in thermal environments. As a result, GLARE shows stress relaxation in the cure cycles during manufacturing the integrated fuselage panel. However, despite the extended research on the material improvements [3–7], the viscoelastic response of GLARE has not been considered yet.

The cure, thermal and viscoelastic properties of Epoxy FM-94, used in prepreg layers of GLARE, are already characterised by the authors in previous works. The material response was needed as the input to the model for predicting the residual stresses after cure cycles of GLARE panels. Consequently, the thermo-elastic and thermo-viscoelastic response of the adhesive in GLARE was determined using Thermo-Mechanical Analysis (TMA) and Dynamic-Mechanical Analysis (DMA) [8]. The viscoelastic response of the composite (prepreg) layers of the FML is obtained from the already determined temperature dependent and viscoelastic response of the epoxy adhesive. The Correspondence principle is used together with self-consistent micromechanics equations in Laplace domain and then the time response is obtained by an inverse transform.

These materials may exhibit large deformations due to non-symmetry after the cooling part of the cure cycle. A material modelling procedure is, therefore, developed for large-displacement (but with small strains) analysis of a thermo-viscoelastic orthotropic material. For the first time, a large deformation thermo-viscoelastic material model is formulated and included in a finite element package for different types of geometries and elements. The model combines programming codes written in FORTRAN and MATLAB. The model is implemented in ANSYS UserMat as a new added feature to the finite element package. Analysis is performed with the input material data for GLARE. Results are obtained for deformation of some non-symmetric panels made of GLARE. Comparison with the curvature measurement of the fabricated laminates shows the applicability and accuracy of the model.

2 Theory

In this section, the theoretical formulations of the material model are described. First, the application of the theory of thermo-viscoelasticity is presented for orthotropic materials undergoing large rotations with small strains. The thermo-viscoelastic model will be used for the cooling part of the cure cycle of FMLs. The stresses due to the adhesive curing, i.e. the curing part of the cure cycle (before cooling), are calculated from a cure-dependent elastic solution; a justification of such an assumption will also be described.

2.1 Equations of thermo-viscoelasticity

This subsection will be concise, but the formulation details of a thermo-viscoelastic problem can be found in the previous work [9].

For a linear viscoelastic material, the constitutive equation is written as [10]:

$$\sigma_i(t) = \int_0^t C_{ij}(t-\tau)\frac{\partial_j}{\partial\tau}d\tau \tag{1}$$

c_{ij} is the component of the general relaxation stiffness for an anisotropic material.

If the polymer is thermo-rheologically simple and the temperature is changing over time, then the mechanical strain in Eq. (1) can be replaced by the difference of the total (measurable) strain and the thermal strain:

$$\sigma_i(t) = \int_0^t C_{ij}(T_0,t'-\tau')\frac{\partial\varepsilon_j^{mech.(\tau)}}{\partial\tau}d\tau$$
$$\varepsilon_j^{mech.}(\tau) = \varepsilon_j^{total}(\tau) - \varepsilon_j^{thermal}(\tau) \tag{2}$$

It is known that for thermo-rheologically simple materials, the time-temperature superposition (TTS) principle [11] can be applied. Accordingly, the relaxation stiffness components can be calculated at any temperature $T(t)$ by evaluation the stiffness at a reference temperature but at a reduced time as:

$$C_{ij}(T(t),t) = C_{ij}(T_0,t') \tag{3}$$

In the above equations, T_0 is the reference temperature and the reduced times are defined as:

$$t' = \int_0^t a_T(T_{(t)})d\tau$$

$$\tau' = \int_0^\tau a_T(T_{(t)})d\tau$$

with a_T as the time-temperature shift factor [9,11].

The free thermal strains are $\int_{T_{ref}}^{T(t)} \alpha_j(T)dT$ with $\alpha_j(T)$ as the temperature dependent coefficient of thermal expansion (CTE).

2.2 Large displacement analysis

The formulation presented in [9] was for small strains and small displacements. Under the latter assumption, no distinction was made between the material coordinates and spatial coordinates, between the finite Green strain tensor and infinitesimal strain tensor, and between the second Piola-Kirchhoff stress tensor and the Cauchy stress tensor.

- Strains are related to the gradients of displacement by means of kinematic equations for a large (nonlinear) deformation:

$$\varepsilon_{ij} = \frac{1}{2}(u_{i,j} + u_{j,i} + \sum_{k=1}^{3} u_{k,i} \cdot u_{k,j}) \quad \textbf{(4)}$$

In the above equations, ε_{ij} is the component of the strain vector and $u_i (i = 1,2,3)$ are the three dimensional displacements in x,y,z directions. The terms under summation in Eq. (4) are the nonlinear terms of displacement for a general nonlinear large deformation finite strain problem, in which large rotations and large strains are present.

Recalling from theory of elasticity [12], Different hypotheses for strain-displacement formulation of elastic materials can be summarised as:

- The most general case is the Green (or Green-Lagrange) strain tensor which is defined as the gradient of the displacement field in the 3-D space, e.g. Eq. (4).
- If the components of the displacement gradients are of order ϵ, then the small strain assumption is valid that implies that the terms of order ϵ^2 are negligible in the strains
- If the rotations of the transverse normal $u_{3,i} (i = 1,2,3)$ are moderate (say 10–15°), then they should be included in the strain-displacement relations. This small-strain with moderate-rotations will lead to geometric nonlinearity of the problem. This latter case is considered in this paper, in which the corresponding second Piola- Kirchhoff stresses are computed.

Larger deformations may occur in large panels as a result of non-symmetric layup or usage of splices and doublers as features commonly present in large fuselage panels made from GLARE. It should be noted that large rotations with small strains is the source of geometric nonlinearity which mainly defines the visco-hypoelastic problem.

2.3 Large rotation incremental formulation in a co-rotated frame

It is possible to solve the integral Eq. (2) using a recursive incremental approach. An iterative scheme is computationally effective in the sense that there will be no need for very small time increments to compensate the error due to the linear approximation of strain increments [13]. The relaxation matrix components should be fitted to a Prony series representing the generalised Maxwell model [10,14] to obtain the recursive formulation:

$$C_{ij}(T_0,t) = C_{ij}^{\infty} + \sum_{m=1}^{N_m} C_{ij}^{m} \exp\left(\frac{-t}{\tau_{ij}^{m}}\right) \quad \textbf{(5)}$$

where N_m is the number of Maxwell elements used and C_{ij}^{∞} is the long-term, i.e. rubbery (fully relaxed), stiffness component. Note that the stiffness components in Eq. (5) are evaluated at reference temperature T_0.

In geometrically nonlinear problems, the user material is formulated in a co-rotational frame. Actually, the frame rotates with the material and the variables are calculated in this rotating frame to account for large rotations. Therefore, the constitutive equations are written in terms of the rotated stress, $\Sigma = R^T \sigma R$, in which R is the rotation arising from the polar decomposition of the deformation gradient (F) and σ is the Cauchy stress tensor in the small displacement case. Accordingly, the stress function in Eq. (2), together with Eq. (5), converts to the following form:

$$\Sigma_i(t) = \sum_{m=1}^{N_m} \int_0^t \left[C_{ij}^{\infty} + C_{ij}^{m} \exp\left(-\frac{t'-\tau'}{\tau_{ij}^{m}}\right) \right] (R^T dR) d\tau$$
$$= \Sigma_i^{\infty}(t) + \sum_{m=1}^{N_m} \mathrm{E}_{ij}^{m}(t) \quad \textbf{(6)}$$

$$\mathrm{E}_{ij}^{m}(t) = \int_0^t \left[C_{ij}^{m} \exp\left(-\frac{t'-\tau'}{\tau_{ij}^{m}}\right) (R^T dR) \right] d\tau \quad \textbf{(7)}$$

where, d is the rate of the deformation tensor D and E_{ij}^{m} are the rotated stress terms for each Maxwell element that should be determined recursively. In this stress function, the strain rate in Eq. (2) is replaced by the known Green-Naghdi rate for large deformations. Assuming that the strain rate is constant over the time increment Δt from t_n until t_{n+1}, time integration of the equation for rotated stress will take the form:

$$\mathrm{E}_{ij}^{m}(t_{n+1}) = \exp\left(-\frac{\Delta t'}{\tau_{ij}^{m}}\right) \mathrm{E}_{ij}^{m}(t_n) + \frac{\tau_{ij}^{m}}{\Delta t'} C_{ij}^{m} \left\{ 1 - \exp\left(-\frac{\Delta t'}{\tau_{ij}^{m}}\right) \right\} R^T_{n+\frac{1}{2}} d_{n+\frac{1}{2}} R_{n+\frac{1}{2}} \quad \textbf{(8)}$$

$\Delta t' = \int_{\tau=t_n}^{t_{n+1}} a_T(T_{(\tau)}) d\tau$ is the reduced time increment. If we assume the shift factor is constant in a small time increment, then:

$$\Delta t' = a_T \Delta t \quad \textbf{(9)}$$

In the above equation:

$R_{n+\frac{1}{2}}$ is the rotation tensor after polar decomposition of the middle point deformation gradient $F_{n+\frac{1}{2}} = (F_n + F_{n+1})/2$, where F_n and F_{n+1} stand for the deformation gradients at the beginning and ending of the current incremental solution, respectively.

In actual implementation, the rate of deformation tensor is replaced by the strain increment as:

$$D_{n+\frac{1}{2}}\Delta t \approx \Delta e_{n+\frac{1}{2}}$$

where, e is the nonlinear strain including higher order derivatives of displacement. Using $\Sigma = R^T \sigma R$ and Eq. (8), the recursive equation can be rewritten in terms of the corresponding Cauchy (un-rotated) stress terms, S_{ij}^m, for each Maxwell element:

$$S_{ij}^m(t_{n+1}) = \exp\left(-\frac{\Delta t'}{\tau_{ij}^m}\right) R S_{ij}^m(t_n) R^T + \frac{\tau_{ij}^m}{\Delta t'} C_{ij}^m \left\{1 - \exp\left(-\frac{\Delta t'}{\tau_{ij}^m}\right)\right\} \Delta R_{\frac{1}{2}}^T \Delta e_{n+\frac{1}{2}} \Delta R_{\frac{1}{2}} \quad \textbf{(10)}$$

where:

$$R = R_{n+1} R_n^T$$

$$R_{\frac{1}{2}} = R_{n+1} R_{n+\frac{1}{2}}^T$$

In order to clarify, we remind that S_{ij}^m are terms of the Cauchy stress tensor (σ), while E_{ij}^m are terms of the rotated stress tensor (Σ), both corresponding to each term of the Maxwell series for stiffness, C_{ij}^m.

From Eqs. (6) and (8), the updated i^{th} component of stress in each time increment can be obtained as:

$$\sigma_i(t_{n+1}) = \sigma_i^{\infty}(t_{n+1}) + \sum_{m=1}^{N_m} \sum_{j=1}^{6} \mathrm{E}_{ij}^m(t_{n+1}) \quad \textbf{(11)}$$

Incremental stress may be calculated as:

$$\Delta\sigma_i(t_{n+1}) = \sigma_i(t_{n+1}) - \sigma_i(t_n) = \left[C_{ij}^{\infty} + \sum_{m=1}^{N_m} \frac{\tau_{ij}^m}{\Delta t^{prime}} C_{ij}^m \left\{1 - \exp\left(-\frac{\Delta t^{prime}}{\tau_{ij}^m}\right)\right\}\right] \Delta R_{\frac{1}{2}}^T \Delta e_{n+\frac{1}{2}} \Delta R_{\frac{1}{2}} + \sum_{m=1}^{N_m} \left\{\exp\left(-\frac{\Delta t^{prime}}{\tau_{ij}^m}\right) - 1\right\} S_{ij}^m(t_{n+1}) \quad \textbf{(12)}$$

Therefore, the stress vector components are updated adding the right hand side of Eq. (12) to the stress value from the previous time increment. In this way, the stresses are calculated in the co-rotated frame and returned at the end of each incremental solution

The consistent tangent stiffness matrix relates incremental stresses to incremental strains. In small displacement formulation, the terms in brackets in Eq. (12) denote the tangent stiffness (material Jacobian matrix) which should be rotated here in the co-rotated frame at the end of each increment:

$$C_{ij}^{\tan} = R_{n+1} \left[C_{ij}^{\infty} + \sum_{m=1}^{N_m} \frac{\tau_{ij}^m}{\Delta t'} C_{ij}^m \left\{1 - \exp\left(-\frac{\Delta t'}{\tau_{ij}^m}\right)\right\}\right] R_{n+1}^T \quad \textbf{(13)}$$

The finite element simulation software needs the above time dependent Jacobian to calculate the strain values for the next time increment.

2.4 Curing stresses

A model was already developed for prediction of residual stresses due to the curing process which consists of chemical deformations and solidification of the epoxy adhesive. The analytic solution presented by the authors in [15] is used here for the calculation of residual stresses during the cure cycle. The thermo-viscoelastic material model developed and presented so far in this paper will be used for the thermal (cooling) part of the cure cycle.

Fig. 1 shows the cure development within a standard cure cycle of GLARE based on cure kinetics measurements. Thermo-Mechanical Analysis (TMA) was also performed in [8] on fully cured samples of the epoxy, as the final T_g was found to be about 92 °C. In cross-linked polymers like epoxy thermosets, the glass transition increases by the polymerisation crosslinking during curing and reaches the final cured value (see e.g. Ref. [16]). Therefore, the epoxy is mainly cured above T_g while the epoxy is in its rubbery state with negligible stress relaxation. Therefore, stress relaxation does not influence the residual stresses during the isothermal curing part and will be considered only during the cool-down part in which the residual stresses are mostly generated. Around the glass-transition temperature, properties including the stiffness and CTE of the prepreg change significantly with temperature. For more details about

obtaining these mechanical and thermal properties, see Ref. [8].

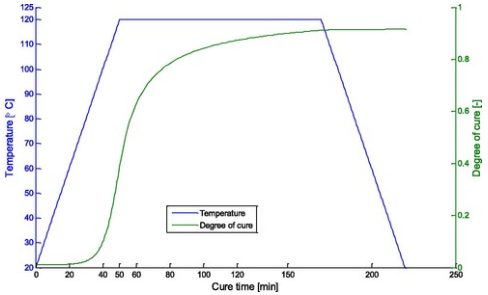

Fig. 1 Temperature and degree of cure during the cure cycle of GLARE [8].

3 Material modelling parameters for GLARE

The work presented in [9] by the authors, was for thermo-viscoelastic analysis of composite (orthotropic) materials within small deformations. Here, the procedure is applied to GLARE material undergoing small and also large displacements (curvature due to the cure cycle). The GLARE laminates are used in fuselage panels of Airbus A-380. The material model described above, is written within a Fortran subroutine to be used by ANSYS finite element package. A generally applicable FE model is beneficial for this type of panels, due to the special and geometrically complex features of fuselage panels made from FMLs including thickness changes, splices, doublers and stringers (see Fig. 2). Splices are used to attach adjacent panels and make larger fuselage panels. Reinforcements like stringers which are used to stiffen the panel for buckling and stability and also large doublers may be bonded to the panel in 2nd cure cycle. The presented procedure in this paper can be used for these features as well. Furthermore, the modelling procedure presented here, can be used for thermal environments other than the curing cycle. For instance one can refer to the thermal cycling happening during the flight of an aeroplane in which thermal effects are present together with the viscoelastic response.

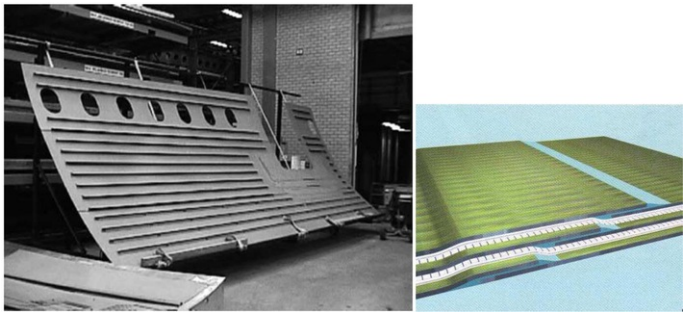

Fig. 2 A fuselage panel made from FMLsleft: cut-outs, doublers and stringers & right: overlap splice between adjacent panels.

The preperg material used in the manufacturing of GLARE, has time-temperature dependent response during the cure cycle. Therefore, change of properties during cure and also the stress relaxation of GLARE at high temperatures, specially near the glass transition of the epoxy adhesive, need to be considered in the residual stress analysis.

3.1 Input material properties

The input material properties for the adhesive polymer (epoxy FM-94) need to be characterised. The curing, thermal and viscoelastic responses of the adhesive are measured during the cure cycle. Differential Scanning Calorimetry (DSC) provided the information about the cure kinetics of the polymer. As a result, evolution of the cure was measured versus time and temperature Dynamic-Mechanical Analysis (DMA) [11] was used in torsional and tensile modes for uncured and fully cured states of the material, respectively. Thermo-Mechanical Analysis (TMA) was used to determine the change of thermal expansion coefficient of the fully cured epoxy adhesive. The authors have already determined the cure-dependent, temperature dependent and viscoelastic responses of the material adhesive of which the details can be found in Ref. [8]. Epoxy FM-94 is used in the fibre layers and also for adhesive bonding of stringers and doublers.

3.2 Fibre Metal Laminate properties

In GLARE, some constituents like the glass fibre and the metal layers behave elastic in the temperature range of the cure cycle (20–120 °C). For the elastic response of the S2-glass/FM94-epoxy prepreg layers, self-consistent micromechanics are used to determine the equivalent layer properties (for the equations see the appendix of Ref. [17]). For the parts of the cure cycle in which the material behaves viscoelastic, the same micromechanics equations are used but in Laplace domain after Laplace transforming of the stiffness of the fibres and the matrix (Correspondence principle). After calculating the stiffness components of the composite in the Laplace domain, the time dependent stiffness components of the prepreg (laminate) can be determined by an inverse Laplace transform. The final solutions are fitted to a generalised Maxwell model in Eq. (5) to be used in the recursive formulation. For a detailed description of the procedure, used for calculating the relaxation stiffness components of the composite laminate, refer to Ref. [9]. For the details of the constituents' properties and the calculations for the laminate response in elastic and viscoelastic (temperature-dependent) regions, the reader can refer to the authors' previous paper [18]. There, you can find the thermo-viscoelastic response of the prepreg plies of GLARE which is calculated from the corresponding viscoelastic properties of the epoxy and elastic properties of the glass fibre.

3.3 Finite element implementation

General-purpose Finite Element Analysis (FEA) packages are capable of modelling complex geometries and features of composites and hybrid materials like FMLs. Layered shell, solid shell and 3-D solid elements can be used for the modelling of different parts of the structure [19]. FE programs, in general, do not have anisotropic viscoelasticity. ANSYS material subroutine (UserMat) is modified for this purpose in Fortran 12.1. Eqs. (10) and (12) are used together with the fitted Prony series in Eq. (5) for each stiffness component of the laminate. The new material model defined for the package makes it possible to analyse thermo-viscoelastic problems in structures which consist of thermoset polymers and/or composites. Large displacements of the structure is implemented in the formulation. For composite and FML panels undergoing large curvatures, the modelling can work with different element types for different parts. Note that no laminate theory is used in the material model. Use of the appropriate theory like first-order shear deformation theory (like in shell or solid-shell elements) or 3-D elasticity equations (in case of continuum solid elements), is determined by how the FE model of the structure is made. In other words, any laminate theory can be used, depending on the selected element type.

The subroutine is called at each element integration point [20], along with which the incremental and total values of the variables are passes into the subroutine from the previous increment. The variables include the deformation, stress and state variables. State variables are those updated recursively at each increment and are defined depending on the formulation of the problem. In our case, state variables are the $S_{ij}^{m}(t)$ terms which denote the stress values for each Maxwell element of the stiffness component. The stresses are updated at each increment within the subroutine and uses the stress values from the previous increment, as in Eq. (12). Deformations are updated using the Jacobian matrix which is defined and updated at each increment within the subroutine.

To ensure overall numerical stability, the integration process should be stable. ANSYS uses a full Newton-Raphson method for the global solution to achieve a better convergence rate. The material Jacobian matrix should be consistent with the material constitutive integration scheme [20]. For this purpose, Eq. (13) is used for the definition of the Jacobian matrix. It should be noted that thermal strains in ANSYS are subtracted from the total strains; therefore, the strains passed to UserMat are the mechanical strains only [20].

4 Results and model verification

Four GLARE panels are manufactured with non-symmetric layups which deformed after cooling. Different amounts of deflection for different panels are obtained that may include small or large rotations and are selected for verification of the predictions from the large-displacement model.

The deflections are measured using Digital Image Correlation (DIC) method. DIC gives a complete three dimensional surface of the deformed panel, in which a 3D image of the panel is gained using two cameras. The cameras have resolution of 4 Megapixels while subsets of about 40 pixels were used in the DIC. Therefore, the final resolution of the DIC measurement would be 6.4 Gigapixels. First the cameras are fixed on mountings, focusing to the object with angle of 30-60°. The cameras are calibrated by a specific calibration sample. As shown in Fig. 3, the panels are painted with white spray and then speckled by black dots (speckle pattern of 3 by 3 pixels).

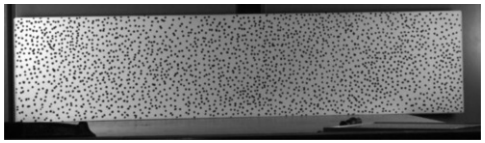

Fig. 3 Large non-symmetric GLARE specimens.

Since the panel is layered and thin, both layered shell and solid-shell elements can be used for finite element modelling. Here, analysis is carried out by a 3-dimensional solid shell element, Solsh190 in ANSYS. This type of element is useful to have a good approximation due to the transverse shear effects and also stresses through the thickness. Having 8 nodes with translational degrees of freedom, Solsh190 elements may be used for simulation of shell

structures with a wide range of thickness (from thin to moderately thick) [19]. A finite element convergence assessment was made on the model from which square elements of 2 cm size led to the most accurate and fast results for deflection.

It is conventional to use a temperature-independent thermo-elastic model to design panels made of GLARE, which uses the thermal properties of the material at room temperature. However, the temperature-dependent thermo-elastic model accounts for the change of coefficient of thermal expansion from cure to room temperature, assuming the cure temperature as the reference for calculation of thermal strains. In thermo-elastic modelling, no stress relaxation is considered. Both the thermo-elastic and thermo-viscoelastic models are used to predict the deformation of non-symmetric panels made of GLARE. The results are improved by adding the stress relaxation. For each panel, small displacement and large-displacement formulations are used for comparison. The results for deflection of panels are gathered in Table 1. As it can be seen from Table 1, large displacement formulation is needed to be accounted for in both thermo-elastic and thermo-viscoelastic models, for panels undergoing large rotations. For panels 1 and 2, since the rotational terms of the deformation are small, the large rotation terms in the formulation are negligible and there is not much difference between the results from the small-displacement and large-displacement formulations. However, for panel 3 and specifically for panel 4 with large rotations, the difference becomes considerable. Furthermore, as it can be seen, adding the curing stresses have improved the model predictions.Table 2

Table 1 Comparison of deflection for largely-deformed GLARE panel.

Mid-span deflection (mm)	ANSYS Temp-dependent Thermo-elastic small-displacement	ANSYS Temp-dependent Thermo-elastic large-displacement	Current model Thermo-viscoelastic small-displacement	Current model Thermo-viscoelastic large-displacement	Current model Thermo-viscoelastic large-displacement + Curing stresses	Measurement
Panel-1 (300 × 30 mm) Al-$[0]_3$-Al-$[90]_3$-Al	6.0	6.0	4.3	4.3	4.1	3.9
Panel-2 (470 × 23 mm) Al-$[0]_3$-Al-$[90]_3$-Al	16.1	16.1	11.6	11.5	11.0	10.8
Panel-3 (378 × 189 mm) Al-$[0]_2$-Al-$[90]_2$-Al	7.5	5.8	6.0	5.4	5.3	5.4
Panel-4 (980 × 220 mm) Al-$[0]_3$-Al-$[90]_3$-Al	73.1	46.0	52.1	28.5	27.7	27.8

For all specimens: Aluminium thickness: 0.4 mm; Prepreg thickness: 0.127 mm.

Table 2 longitudinal mid-layer stresses in a typical non-symmetric GLARE panel.

Layer	Al	0°	0°	0°	Al	90°	90°	90°	Al
Residual Stresses [MPa]	31.8	−57.4	−59.7	−62.0	15.9	9.6	9.5	9.3	0.1

For the illustration purpose, the deformed shape of Panel-4 is measured by DIC and shown in Fig. 4 which can be compared to Fig. 5 which shows the result from the current large-displacement model including the curing stresses. As it can be observed, the model shows accurate predictions for both the maximum deflection and also the deformation pattern.

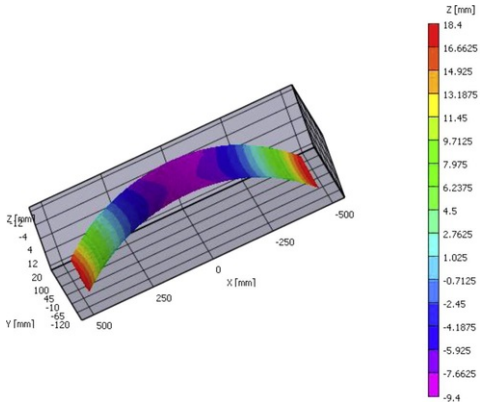

Fig. 4 Deformation of panel-4 measured by DIC (δ_{max} = 18.4 + 9.4 = 27.8 mm).

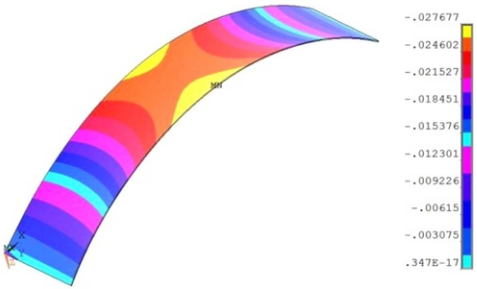

Fig. 5 Deformation of panel-4 by the current model including curing stresses (values are in meter, δ_{max} = 27.7 mm).

As the second illustrative example, the deformation of panel-3 can be seen in Fig. 6, from DIC measurement and in Fig. 7, from the current modelling procedure including the curing stresses. Note that the deformation contour in Fig. 6 should be scaled by a factor of 1.5 due to a scaled calibration used in the DIC measurement.

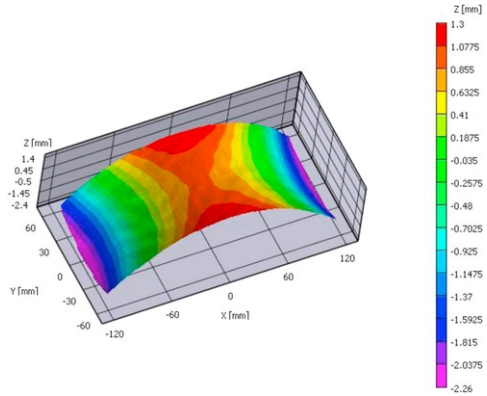

Fig. 6 Deformation of panel-3 measured by DIC (δ_{max} = 3.6 * 1.5 = 5.4 mm; δ_{mid} = 3.2 * 1.5 = 4.8 mm).

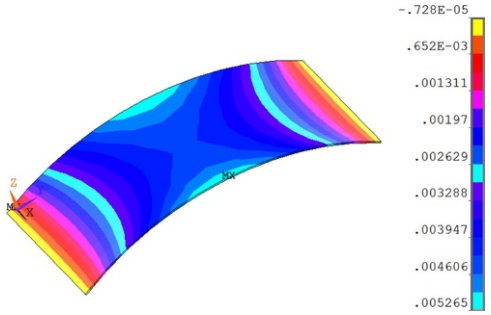

Fig. 7 Deformation of panel-3 the current model including curing stresses (values are in meter, δ_{max} = 5.3 mm).

It should be noted that the current results are for deflection. In the next stage of research, measurement of residual stresses and comparison with modelling can be performed to have a model capable of predicting both warpage and residual stresses with an acceptable accuracy. As an example, see Table for the layers' residual stresses in a typical FML in which the laminate has a non-symmetric layup of (Al-$[0]_3$-Al-$[90]_3$-Al).

As it can be seen, the residual stresses are considerable in the layers. Especially, the residual stresses in the Aluminium layers are tensile and have large amounts which are of high importance in the fatigue life. Since, the initiation of fatigue occurs in the metal layers of FMLs, reduction of tensile stresses will have major role in the life of the fuselage panels. Therefore, reduction of the stresses could be an idea for continuing this research. This may be carried out by changing the design parameters and also the cure cycle parameters.

5 Conclusion

A geometrically nonlinear material model was implemented in ANSYS UserMat for temperature dependent viscoelastic modelling of orthotropic laminates including the curing stresses. Thermo-viscoelastic properties of GLARE were determined from elastic and viscoelastic properties of the GLARE constituents. Curing stresses were calculated from an analytical model for cure-induced residual stresses and deflections of an orthotropic material and were included in the predictions as initial stresses. The accuracy of the formulated model was checked by comparing to fabricated non-symmetric GLARE panels with large curvatures. It was shown that the stress relaxation and large rotational strains should be considered for an accurate prediction of residual stresses and distortions of non-symmetric GLARE panels. The model together with the time-temperature dependent response of the epoxy adhesive and the prepreg layers can be used for analysis of featured panels made from GLARE (with cut-outs and doublers) in future phases of research in any application in which time and/or temperature change is of concern. The modelling procedure is extendable to structural parts with any type of geometry made from orthotropic materials under small or large deformations.

References

[1] M. Abouhamzeh, J. Sinke and R. Benedictus, On the prediction of cure-induced shape deviations in fiber metal laminates, *J Compos Mater* **49**, 2015, 1705–1716.

[2] M. Abouhamzeh, J. Sinke and R. Benedictus, Investigation of curing effects on distortion of fibre metal laminates, *Compos Struct* **122**, 2015, 546–552.

[3] A. Asundi and A.Y.N. Choi, Fiber metal laminates: An advanced material for future aircraft, *J Mater Process Technol* **63**, 1997, 384–394.

[4] R.C. Alderliesten, Fatigue crack propagation and delamination growth in glare, 2005, Delft University of Technology; The Netherlands.

[5] J.J. Homan, Fatigue initiation in fibre metal laminates, *Int J Fatigue* **28**, 2006, 366–374.

[6] J. Sinke, Development of Fibre Metal Laminates: concurrent multi-scale modeling and testing, *J Mater Sci* **41**, 2006, 6777–6788.

[7] R.C. Alderliesten and R. Benedictus, Fiber/metal composite technology for future primary aircraft structures, *J Aircr* **45**, 2008, 1182–1189.

[8] M. Abouhamzeh, J. Sinke, K.M.B. Jansen and R. Benedictus, Kinetic and thermo-viscoelastic characterization of the epoxy adhesive in GLARE, *Compos Struct* **124C**, 2015, 19–28.

[9] M. Abouhamzeh, J. Sinke, K.M.B. Jansen and R. Benedictus, A new procedure for thermo-viscoelastic modelling of composites with general orthotropy and geometry, *Compos Struct* **133**, 2015, 871–877.

[10] N.W. Tschoegl, The phenomenological theory of linear viscoelastic behavior, an introduction, 1989, Springer-Verlag; Berlin, Germany.

[11] Menczel JD, Prime RB. Thermal analysis of polymers: fundamentals and applications, 2008.

[12] J.N. Reddy, Mechanics of laminated composite plates and shells, 2004, CRC Press; New York.

[13] S. Sawant and A. Muliana, A thermo-mechanical viscoelastic analysis of orthotropic materials, *Compos Struct* **83**, 2008, 61–72.

[14] E. Riande, R. Diaz-Calleja, M. Prolongo, R. Masegosa and C. Salom, Polymer viscoelasticity: stress and strain in practice, 1st ed., 2000, Marcel Dekker; New York.

[15] M. Abouhamzeh, J. Sinke, K.M.B. Jansen and R. Benedictus, Closed form expression for residual stresses and warpage during cure of composite laminates, *Compos Struct* **133**, 2015, 902–910.

[16] M. Sadeghinia, K.M.B. Jansen and L.J. Ernst, Characterization of the viscoelastic properties of an epoxy molding compound during cure, *Microelectron Reliab* **52**, 2012, 1711–1718.

[17] T.A. Bogetti and J.W. Gillespie, Process-induced stress and deformation in thick-section thermoset composite laminates, *J Compos Mater* **26**, 1992, 626–660.

[18] M. Abouhamzeh, J. Sinke, K.M.B. Jansen and R. Benedictus, Thermo-viscoelastic analysis of GLARE, *Compos B* **99**, 2016, 1–8.

[19] ANSYS. Mechanical APDL Theory Reference. ANSYS® Academic Research, Help System, Release 15.0; 2014.

[20] ANSYS. Guide to User-Programmable Features. ANSYS® Academic Research, Help System, Release 15.0; 2014.